

A Study of the Transition Between Metastable States of Droplets on Superhydrophobic Surfaces

Kellen Petersen

Department of Mathematics
Courant Institute of Mathematical Sciences
New York University

National Institute of Standards and Technology
Gaithersburg, Maryland
July 30, 2012



Outline

1 Background

Outline

- 1 Background
- 2 Pillared Surfaces
 - Method and Implementation
 - Results
 - Minimum Energy Paths

Outline

- 1 Background
- 2 Pillared Surfaces
 - Method and Implementation
 - Results
 - Minimum Energy Paths
- 3 Chemically Structured Surfaces
 - 2D & 3D Results

Outline

- 1 Background
- 2 Pillared Surfaces
 - Method and Implementation
 - Results
 - Minimum Energy Paths
- 3 Chemically Structured Surfaces
 - 2D & 3D Results
- 4 Conclusions and Future Work
 - Conclusion
 - Future Work

Introduction

The Lotus Effect



Photo Credit: Flickr (tanakawho)
Inset: V. Zorba, et al. Adv. Mater. 20, pp. 4049-4054.

Introduction

The Lotus Effect

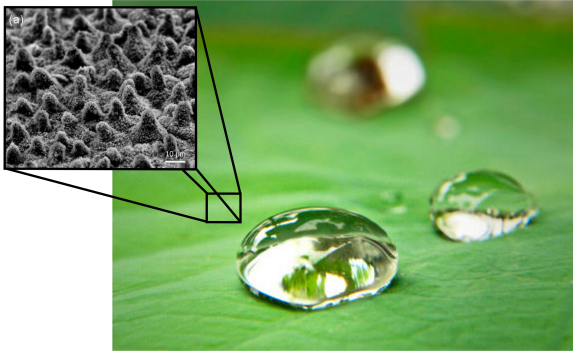
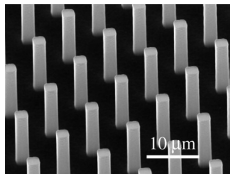


Photo Credit: Flickr (tanakawho)
Inset: V. Zorba, et al. Adv. Mater. 20, pp. 4049-4054.

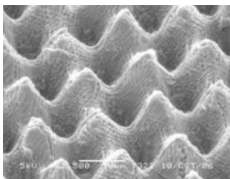
Introduction to Pillared Surfaces



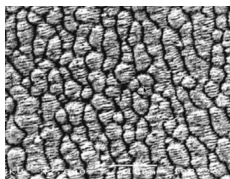
Lotus Plant



Mechanically Pillared



Pillar-Like Surface



Self-Organizing Surface

Top Left:

Photo Credit: Flickr (tanakawho)

Top Right:

Quéré, et al. Phil. Trans. R. Soc. A 13, vol. 366, no. 1870, 1539-1556

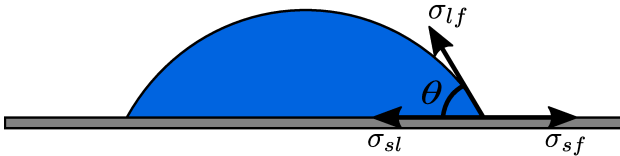
Bottom Left:

M. Groenendijk, Self-cleaning plastic modeled on leaf, Discovery News (2007). Impact, IPV, EM

Bottom Right:

Römer, et al. CIRP Annals, 58, 201-204 (2009)

Young's Relation



σ_{sl} = solid-liquid

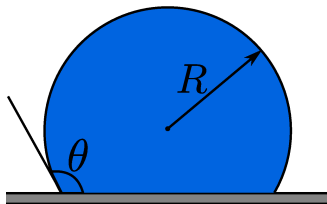
σ_{sf} = surface-fluid

σ_{lf} = liquid-fluid

Young's Relation (1905)

$$\cos \theta_Y = \frac{\sigma_{sf} - \sigma_{sl}}{\sigma_{lf}}$$

Capillary Length



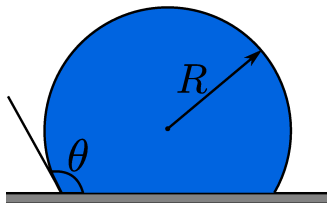
Surface Energy
scales as $\sigma_{lf}R^2$

$$\sigma_{lf}R^2 \gg \Delta n g R^4$$

Gravitational Energy
scales as $\Delta n g R^4$

$$\lambda_C = \sqrt{\frac{\sigma_{lf}}{\Delta n g}}$$

Capillary Length



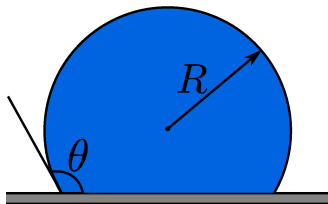
Typical Values

$$\sigma_{lf} \approx 10^{-2} \text{ N} \cdot \text{m}^{-1}$$

$$\Delta n \approx 10^3 \text{ kg} \cdot \text{m}^{-3}$$

$$g \approx 10 \text{ m} \cdot \text{s}^{-2}$$

Capillary Length



Typical Values

$$\sigma_{lf} \approx 10^{-2} \text{ N} \cdot \text{m}^{-1}$$

$$\Delta n \approx 10^3 \text{ kg} \cdot \text{m}^{-3}$$

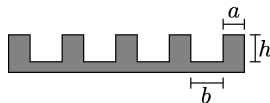
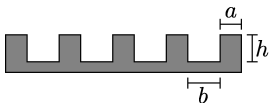
$$g \approx 10 \text{ m} \cdot \text{s}^{-2}$$



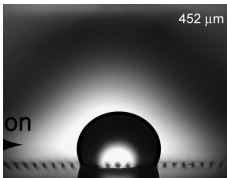
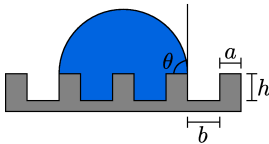
$$\lambda_C \approx 1 \text{ mm}$$

Droplets Size
 $\approx 10 - 100 \mu\text{m}$

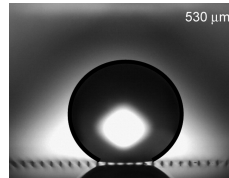
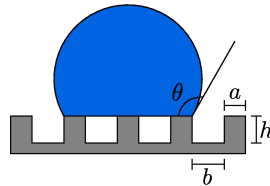
Superhydrophobic Surfaces



Superhydrophobic Surfaces



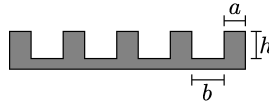
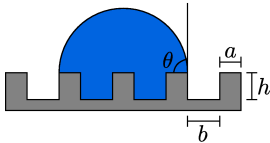
Wenzel State



Cassie-Baxter State

Experimental Images: Nosonovsky et al. Langmuir, 2008, 24 (4), pp 1525-1533

Superhydrophobic Surfaces

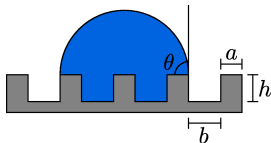


Wenzel (1936)

r = Roughness Ratio

$$\cos \theta_W = r \cos \theta_Y$$

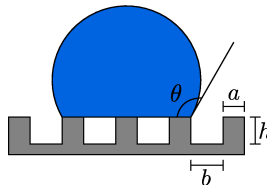
Superhydrophobic Surfaces



Wenzel (1936)

r = roughness ratio

$$\cos \theta_W = r \cos \theta_Y$$



Cassie-Baxter (1940)

r_f = roughness ratio of wet area

f = fraction of solid area wet

$$\cos \theta_{CB} = r_f f \cos \theta_Y - (1 - f)$$

Note: When $f = 1$ and $r_f = r$ the CB equation reduces to the Wenzel equation

Gibbs Energy

In general, we can write the Gibbs free energy for a penetrating drop on a textured surface as

$$G = \sigma_{lv}A_{lv} + \sigma_{ls}A_{ls} + \sigma_{vs}A_{vs}$$

Assumptions:

- Droplet forms a spherical cap (no gravity)
- Radius of curvature in the pores is same as for the droplet (interface is approximately planar)
- Volume in the pores is negligible
- Projected liquid-solid area is approximately equal to base area of spherical cap

Based on formulation of Marmur, Langmuir 19, 8343-8348 (2003)

Gibbs Energy

In general, we can write the Gibbs free energy for a penetrating drop on a textured surface as

$$G = \sigma_{lv}A_{lv} + \sigma_{ls}A_{ls} + \sigma_{vs}A_{vs}$$

where we use the following equations

$$A_{lv} = 2\pi R^2(1 - \cos \theta) + (1 - f)\pi R^2 \sin^2 \theta$$

$$A_{ls} = \pi R^2 r_f f \sin^2 \theta$$

$$A_{vs} = [A_{total} - \pi R^2 r \sin^2 \theta] \pi R^2 r_{1-f} (1 - f) \sin^2 \theta$$

$$r = r_f f + r_{1-f} (1 - f)$$

Gibbs Energy

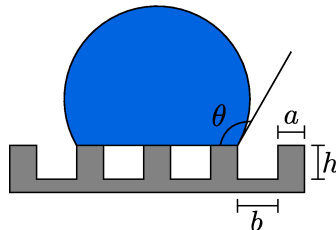
Normalizing the energy ($G^* = \frac{G}{\sigma_{lv}\pi^{1/3}(3V)^{2/3}}$) we have

$$G^* = F^{-2/3}(\theta) [2 - 2 \cos \theta - \Phi(f) \sin^2 \theta]$$

where

$$F(\theta) = 2 - 3 \cos \theta + \cos^3 \theta$$

$$\Phi(f) = r_f f \cos(\theta_Y) + f - 1$$



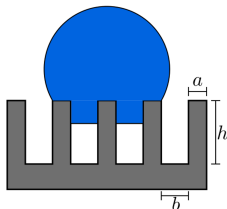
Gibbs Energy Landscape

Assuming a flat advancing interface:

$$f = \frac{a}{a+b}, \quad r_f = \frac{a+h}{a}$$

$$a = b = 0.3, \quad h = 1$$

$$\theta_Y = 110^\circ$$



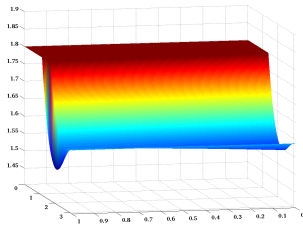
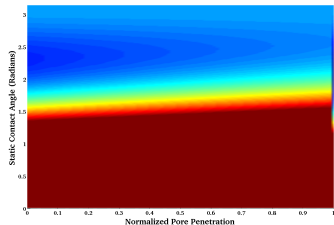
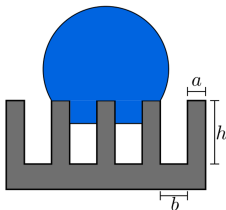
Gibbs Energy Landscape

Assuming a flat advancing interface:

$$f = \frac{a}{a+b}, \quad rf = \frac{a+h}{a}$$

$$a = b = 0.3, \quad h = 1$$

$$\theta_Y = 110^\circ$$



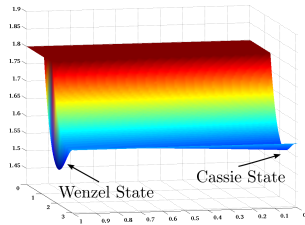
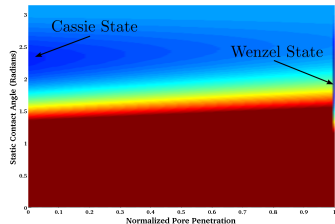
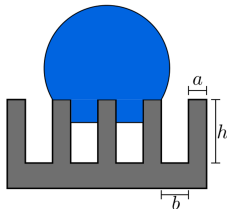
Gibbs Energy Landscape

Assuming a flat advancing interface:

$$f = \frac{a}{a+b}, \quad rf = \frac{a+h}{a}$$

$$a = b = 0.3, \quad h = 1$$

$$\theta_Y = 110^\circ$$



Gibbs Energy Landscape

Assuming a curved advancing interface:

$$f = \begin{cases} \frac{a}{a+b}, & \text{if } p < p^* \\ \frac{a + \sqrt{d(2R-d)}}{a+b}, & \text{if } p > p^* \end{cases}$$

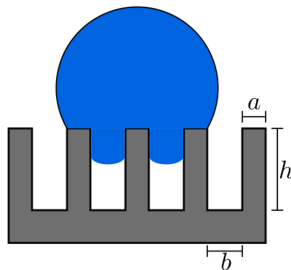
$$r_f = \begin{cases} \frac{a+h}{a}, & \text{if } p < p^* \\ \frac{a+h + \sqrt{d(2R-d)}}{a + \sqrt{d(2R-d)}}, & \text{if } p > p^* \end{cases}$$

$$d = (f - 1)h + R(1 - \cos(\theta_Y - \frac{\pi}{2}))$$

$$R = a / \sin(\theta_Y - \frac{\pi}{2})$$

$$a = b = 0.3, \quad h = 1$$

$$\theta_Y = 110^\circ$$



Gibbs Energy Landscape

Assuming a curved advancing interface:

$$f = \begin{cases} \frac{a}{a+b}, & \text{if } p < p^* \\ \frac{a + \sqrt{d(2R-d)}}{a+b}, & \text{if } p > p^* \end{cases}$$

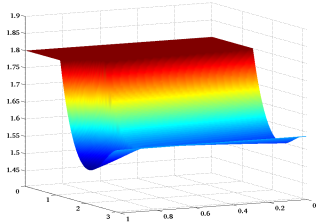
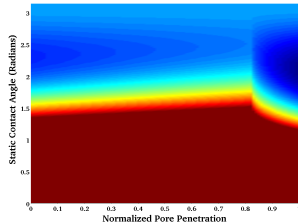
$$r_f = \begin{cases} \frac{a+h}{a}, & \text{if } p < p^* \\ \frac{a+h + \sqrt{d(2R-d)}}{a + \sqrt{d(2R-d)}}, & \text{if } p > p^* \end{cases}$$

$$d = (f - 1)h + R(1 - \cos(\theta_Y - \frac{\pi}{2}))$$

$$R = a / \sin(\theta_Y - \frac{\pi}{2})$$

$$a = b = 0.3, \quad h = 1$$

$$\theta_Y = 110^\circ$$



Gibbs Energy Landscape

Assuming a curved advancing interface:

$$f = \begin{cases} \frac{a}{a+b}, & \text{if } p < p^* \\ \frac{a + \sqrt{d(2R-d)}}{a+b}, & \text{if } p > p^* \end{cases}$$

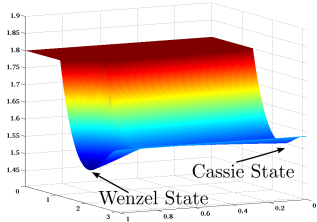
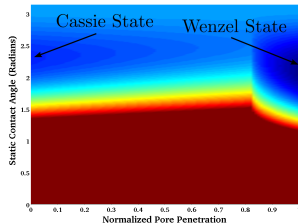
$$r_f = \begin{cases} \frac{a+h}{a}, & \text{if } p < p^* \\ \frac{a+h + \sqrt{d(2R-d)}}{a + \sqrt{d(2R-d)}}, & \text{if } p > p^* \end{cases}$$

$$d = (f - 1)h + R(1 - \cos(\theta_Y - \frac{\pi}{2}))$$

$$R = a / \sin(\theta_Y - \frac{\pi}{2})$$

$$a = b = 0.3, \quad h = 1$$

$$\theta_Y = 110^\circ$$



Phase Field Method

Consider a bounded region $\Omega \in \mathbb{R}^d$ where $d = 2, 3$. We then use a Cahn-Hilliard energy functional

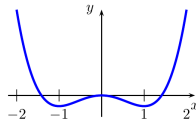
$$E(\phi) = \int_{\Omega} \frac{\kappa}{2} |\nabla \phi|^2 + f(\phi) + \phi G(x) dx$$

$G(x)$ = Gravitational Potential

κ = Parameter (Interfacial Width)

$$f(\phi) = \frac{\phi^4}{4} - \frac{\phi^2}{2}$$

Stable phases: $\phi = \pm 1$



Phase Field Method with Surface

Consider a bounded region $\Omega \in \mathbb{R}^d$ where $d = 2, 3$ with boundary $\partial\Omega$. Let Γ be the part of the boundary corresponding to the physical surface. Neglecting gravity, the Cahn-Hilliard energy functional is

$$E(\phi) = \int_{\Omega} \frac{\kappa}{2} |\nabla \phi|^2 + f(\phi) dx - \int_{\Gamma} \gamma_f(\phi) ds$$

$$f(\phi) = \frac{\phi^4}{4} - \frac{\phi^2}{2}$$

$$\gamma_f(\phi) = \Delta\gamma \cdot \sin \frac{\pi}{2} \phi$$

$$\Delta\gamma = \gamma \cos \theta_Y$$

$$\gamma = \frac{2\sqrt{2}}{3} \sqrt{\kappa}$$

Phase Field Method with Surface

Consider a bounded region $\Omega \in \mathbb{R}^d$ where $d = 2, 3$ with boundary $\partial\Omega$. Let Γ be the part of the boundary corresponding to the physical surface. Neglecting gravity, the Cahn-Hilliard energy functional is

$$E(\phi) = \int_{\Omega} \frac{\kappa}{2} |\nabla \phi|^2 + f(\phi) dx - \int_{\Gamma} \gamma_{lf}(\phi) ds$$

$$f(\phi) = \frac{\phi^4}{4} - \frac{\phi^2}{2}$$

$$\gamma_{lf}(\phi) = \Delta\gamma \cdot \sin \frac{\pi}{2} \phi$$

$$\Delta\gamma = \gamma \cos \theta_Y$$

$$\gamma = \frac{2\sqrt{2}}{3} \sqrt{\kappa}$$

$\kappa |\nabla \phi|^2$: Controls surface tension

$f(\phi)$: Bulk term (Van der Waals)

$\gamma_{lf}(\phi)$: Controls contact angle

Controlling the Contact Angle

Minimizing the total free energy with respect to ϕ at the solid surface yields:

$$\left[\kappa \partial_n \phi + \frac{\partial \gamma_{lf}(\phi)}{\partial \phi} \right]_{\phi_{eq}} = 0$$

Therefore, using the above expression for γ_{lf} we get

Controlling the Contact Angle

Minimizing the total free energy with respect to ϕ at the solid surface yields:

$$\left[\kappa \partial_n \phi + \frac{\partial \gamma_{lf}(\phi)}{\partial \phi} \right]_{\phi_{eq}} = 0$$

Therefore, using the above expression for γ_{lf} we get

$$\partial_n \phi = \frac{\pi \Delta \gamma}{4\kappa} \cos \frac{\pi}{2} \phi$$

Gradient Flow

To get the gradient flow equation we set the time derivative equal to negative the first variation of $E(t)$: $-\frac{\delta E}{\delta \phi}$

Gradient Flow

To get the gradient flow equation we set the time derivative equal to negative the first variation of $E(t)$: $-\frac{\delta E}{\delta \phi}$

$$\phi_t = \kappa \Delta \phi - (\phi^3 - \phi) + \lambda \quad x \in \Omega$$

where λ is a lagrange multiplier for the constraint
 $\int_{\Omega} \phi(x) dx = \text{Constant}$

Gradient Flow

To get the gradient flow equation we set the time derivative equal to negative the first variation of $E(t)$: $-\frac{\delta E}{\delta \phi}$

$$\phi_t = \kappa \Delta \phi - (\phi^3 - \phi) + \lambda \quad x \in \Omega$$

$$\partial_n \phi = \frac{\pi \Delta \gamma}{4\kappa} \cos \frac{\pi}{2} \phi \quad \text{on solid surface}$$

$$\partial_n \phi = 0 \quad \text{on other boundaries}$$

where λ is a lagrange multiplier for the constraint

$$\int_{\Omega} \phi(x) dx = \text{Constant}$$

Numerical Implementation

We implement a Forward Euler scheme for the time integration and finite differences with the 5-point Laplacian.

The following splitting scheme is used to determine λ at each timestep.

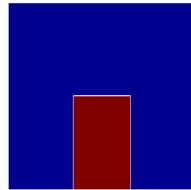
$$\phi^{n+\frac{1}{2}} = \kappa \Delta \phi^n - \phi^n (\phi^n - 1)(\phi^n + 1)$$

$$\lambda^n = -\frac{1}{|\Omega|} \int_{\Omega} \phi^{n+\frac{1}{2}} dx$$

$$\phi^{n+1} = \phi^n + d\tau (\phi^{n+\frac{1}{2}} + \lambda^n)$$

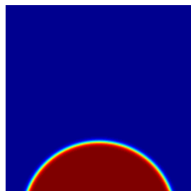
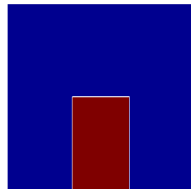
Droplets on Flat Surfaces

Consider the initial
configuration for ϕ .
Solve the system to
steady-state ($t \rightarrow \infty$)

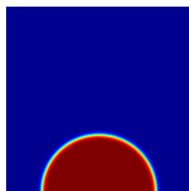


Droplets on Flat Surfaces

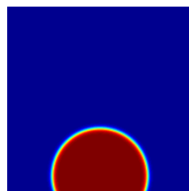
Consider the initial configuration for ϕ .
Solve the system to steady-state ($t \rightarrow \infty$)



$$\theta_Y = 70^\circ$$

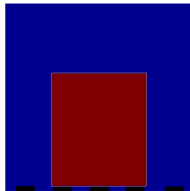


$$\theta_Y = 90^\circ$$

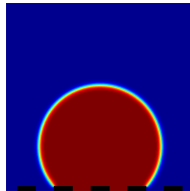


$$\theta_Y = 110^\circ$$

Droplets on Pillared Surfaces



Initial



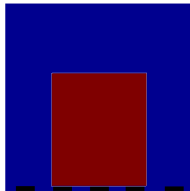
Final

Diffuse-Interface Model

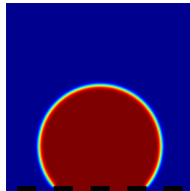
$$\theta_Y = 99^\circ$$

$$h = 0.025, a = b = 0.1$$

Droplets on Pillared Surfaces



Initial

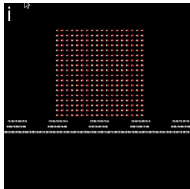


Final

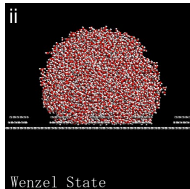
Diffuse-Interface Model

$$\theta_Y = 99^\circ$$

$$h = 0.025, a = b = 0.1$$



Initial



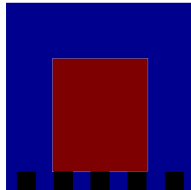
Final

MD Simulations

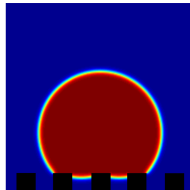
5,832 molecules

* MD Figs: Koishi, et al. PNAS Vol. 106, No. 21, 8435

Droplets on Pillared Surfaces



Initial



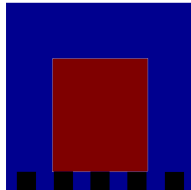
Final

Diffuse-Interface Model

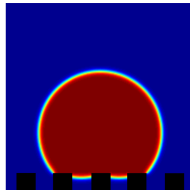
$$\theta_Y = 99^\circ$$

$$h = 0.1, a = b = 0.1$$

Droplets on Pillared Surfaces



Initial

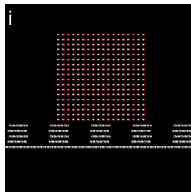


Final

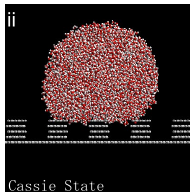
Diffuse-Interface Model

$$\theta_Y = 99^\circ$$

$$h = 0.1, a = b = 0.1$$



Initial



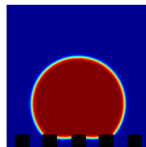
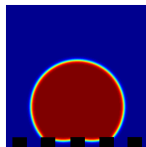
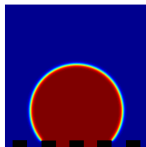
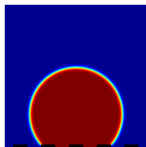
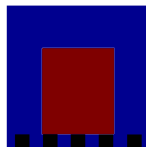
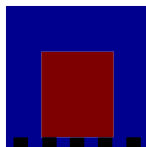
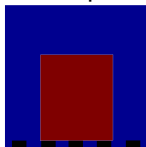
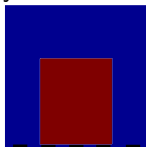
Final

MD Simulations

5,832 molecules

Droplets on Pillared Surfaces

We find there is a critical height such that for short pillars Wenzel is the only stable state. For taller pillars the Cassie-Baxter state is metastable.



$h = 0.025$

$h = 0.05$

$h = 0.075$

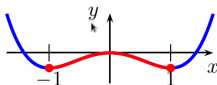
$h = 0.1$

Minimal Energy Paths (MEPs)

Given potential energy $E(\mathbf{x})$ with two energy minima, the MEP is a smooth curve ϕ^* connecting two minima that satisfies $(\nabla E)^\perp(\phi^*) = 0$.

Minimal Energy Paths (MEPs)

Given potential energy $E(\mathbf{x})$ with two energy minima, the MEP is a smooth curve ϕ^* connecting two minima that satisfies $(\nabla E)^\perp(\phi^*) = 0$.

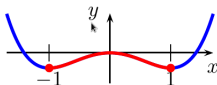


1D Example

$$E(x) = \frac{x^4}{4} - \frac{x^2}{2}$$

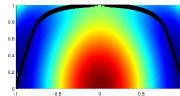
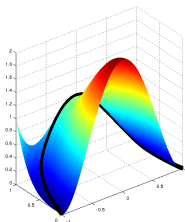
Minimal Energy Paths (MEPs)

Given potential energy $E(\mathbf{x})$ with two energy minima, the MEP is a smooth curve ϕ^* connecting two minima that satisfies $(\nabla E)^\perp(\phi^*) = 0$.



1D Example

$$E(x) = \frac{x^4}{4} - \frac{x^2}{2}$$



2D Example

$$E(x, y) = (x^2 - 1)^2 + (x^2 + y^2 - 1)^2$$

The (Improved) String Method

Given a string $\{\phi_i^0, i = 0, \dots, N\}$

Step 1: Evolve the string

$$\phi_i^* = \phi_i^n - \Delta t \nabla E(\phi_i^n)$$

Step 2: Interpolation and Reparametrization

- Calculate arc length of images

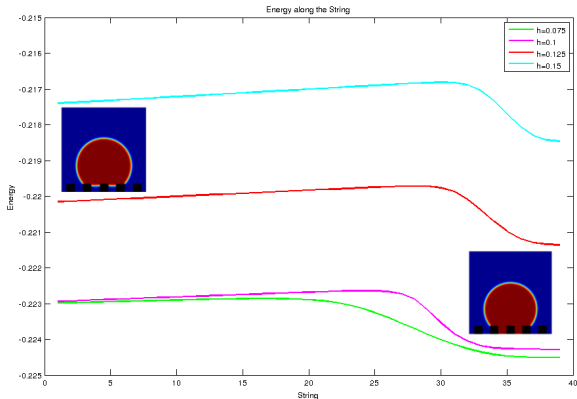
$$s_0 = 0, s_i = s_{i-1} + |\phi_i^* - \phi_{i-1}^*|, i = 1, 2, \dots, N$$

Obtain mesh $\alpha_i^* = s_i/s_N$

- Interpolate new points ϕ_i^{n+1} on uniform grid $\alpha_i = i/N$ using cubic splines.

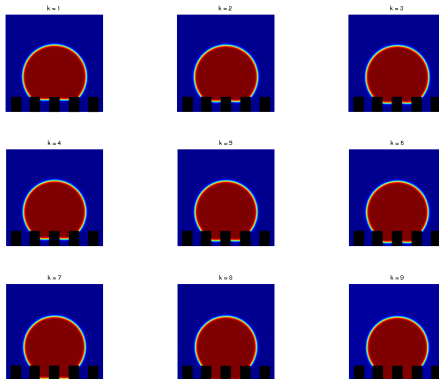
Minimal Energy Path

Using the string method as describe we are able to obtain the following plots of Energy along the MEP for various pillar heights.



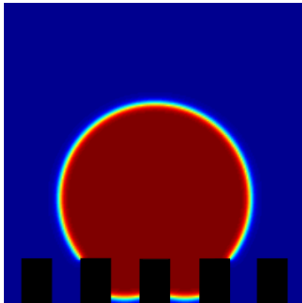
Minimal Energy Path

The **collapse transition** can now be seen by looking at droplet configurations along the minimal energy path.



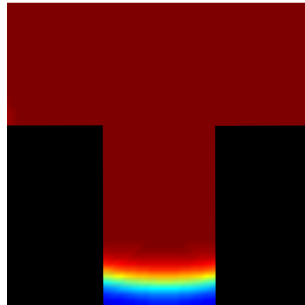
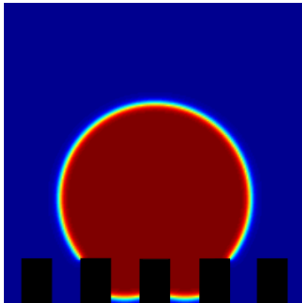
Saddle Point

The **Climbing Image Technique** can be combined with the String Method to find the saddle point configuration along the MEP.



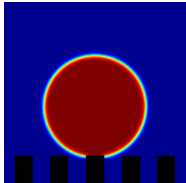
Saddle Point

The **Climbing Image Technique** can be combined with the String Method to find the saddle point configuration along the MEP.

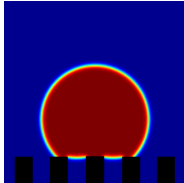


Stable and Metastable States

Stable and Metastable States

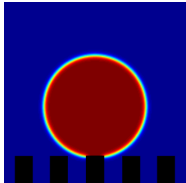


Cassie (1 Pillar)

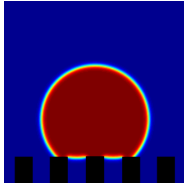


Cassie (3 Pillars)

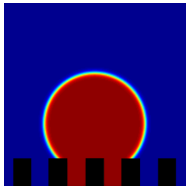
Stable and Metastable States



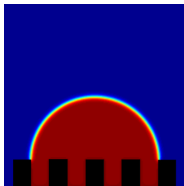
Cassie (1 Pillar)



Cassie (3 Pillars)

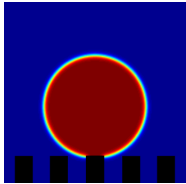


Wenzel (2 Pores)

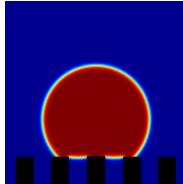


Wenzel (4 Pores)

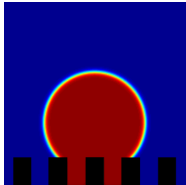
Stable and Metastable States



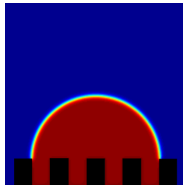
Cassie (1 Pillar)



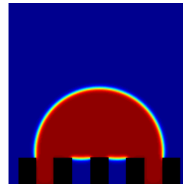
Cassie (3 Pillars)



Wenzel (2 Pores)



Wenzel (4 Pores)



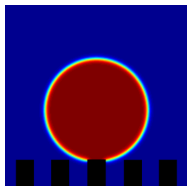
Impregnated

Causes of Energy Barrier

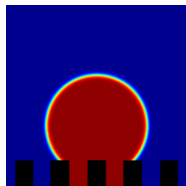
Consider the transition: **Cassie (1 Pillar) to Wenzel (2 Pores)**

Causes of Energy Barrier

Consider the transition: **Cassie (1 Pillar) to Wenzel (2 Pores)**



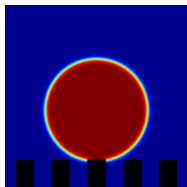
Cassie (1 Pillar)



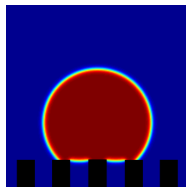
Wenzel (2 Pores)

Causes of Energy Barrier

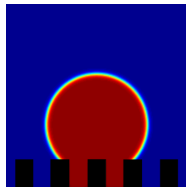
Consider the transition: **Cassie (1 Pillar) to Wenzel (2 Pores)**



Cassie (1 Pillar)



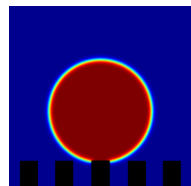
Cassie (3 Pillar)



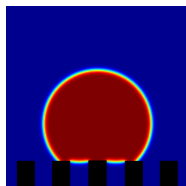
Wenzel (2 Pores)

Causes of Energy Barrier

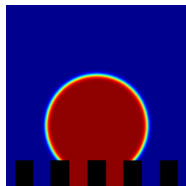
Consider the transition: **Cassie (1 Pillar) to Wenzel (2 Pores)**



Cassie (1 Pillar)



Cassie (3 Pillar)



Wenzel (2 Pores)

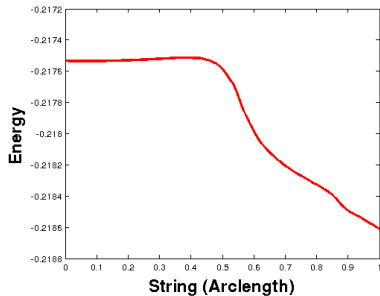
Sources of energy barrier:

- Triple Line Displacement
- Collapse Transition

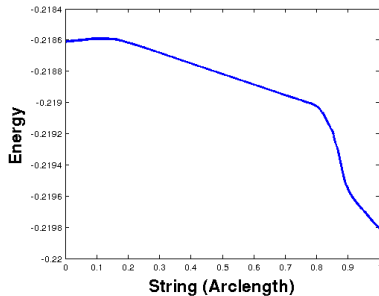
Reference:
Bormashenko
Langmuir 2012

Causes of Energy Barrier

Consider the transition: **Cassie (1 Pillar) to Wenzel (2 Pores)**

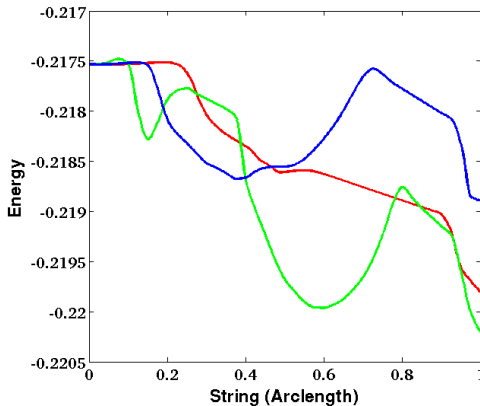


Cassie-1 to Cassie-3



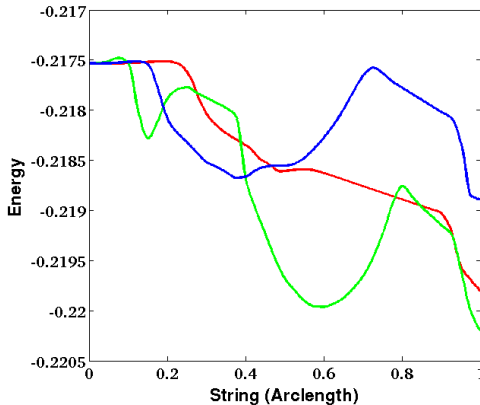
Cassie-3 to Wenzel-2

Cassie to various Collapsed States



Red: C1 to W2
Green: C1 to W4
Blue: C1 to Impregnated

Cassie to various Collapsed States



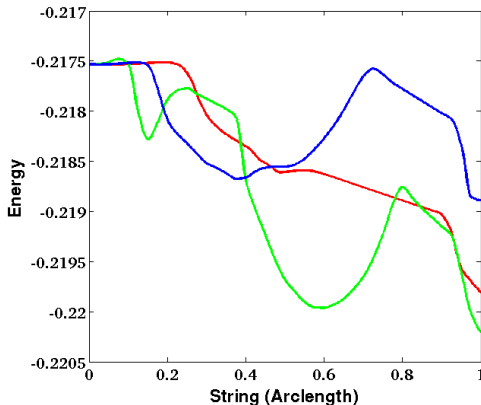
Red: C1 to W2

Green: C1 to W4

Blue: C1 to Impregnated

- W4 is the lowest energy state

Cassie to various Collapsed States



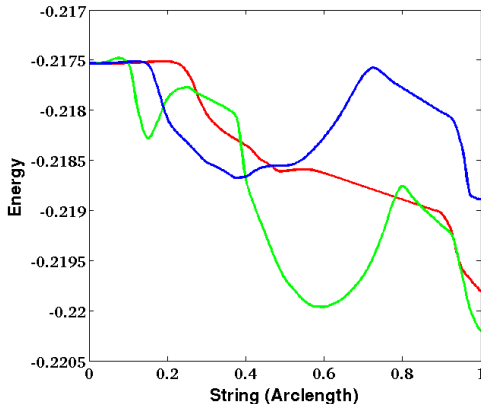
Red: C1 to W2

Green: C1 to W4

Blue: C1 to Impregnated

- W4 is the lowest energy state
- First Cassie state along green has higher energy than others

Cassie to various Collapsed States



Red: C1 to W2

Green: C1 to W4

Blue: C1 to Impregnated

- W4 is the lowest energy state
- First Cassie state along green has higher energy than others
- Intermediate state for red has low energy barrier

Transitions to Different Final States

Let the domain be $[0, 1]^2$ and the surface be **5 pillars** with
 $h = 0.15, a = b = 0.1$ and $\theta_Y = 110^\circ$

Cassie-1
to
Wenzel-2

Cassie-1
to
Wenzel-4

Cassie-1
to
Impregnated

The Collapse Transition

How does a drop collapse on surfaces with many pillars?

Theory and Computation

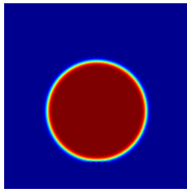
- A **uniform** collapse: 2D analytical results (Kusumaatmaja et. al, *EPL* 2008)
- A **Middle-Out** collapse: Computational Results using Lattice Boltzmann Method (Yeomans' Group, University of Oxford, England)
- An **Out-Middle** collapse: Theoretical Results (Bormashenko Group, Ariel University, Israel)

Experiment

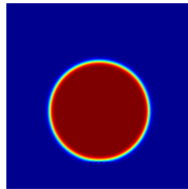
- Applied Voltage to collapse drop **through impregnation** (Bahadur and Garimella, *Langmuir* 2009)
- Various collapse patterns including **Middle-Out** collapses (Moulinet and Bartolo, *Euro. Phys. J. E* 2007)

Transitions to Different Final States (32 Pillars)

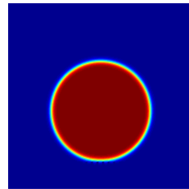
Let the domain be $[0, 1]^2$ and the surface be **32 pillars** with $h = 0.15, a = b = 0.03$ and $\theta_Y = 110^\circ$



Cassie-1
to
Wenzel
(Marching)



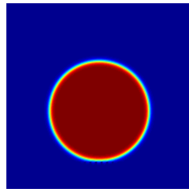
Cassie-1
to
Wenzel
(Showering)



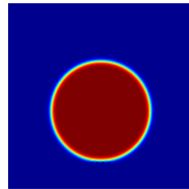
Cassie-1
to
Impregnated

Transitions to Different Final States (32 Pillars)

Let the domain be $[0, 1]^2$ and the surface be **32 pillars** with $h = 0.15, a = b = 0.03$ and $\theta_Y = 110^\circ$



Cassie-1
to
Wenzel
(Marching)

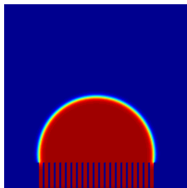


Cassie-1
to
Wenzel
(Showering)

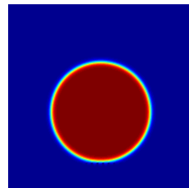
Cassie-1
to
Impregnated

Transitions to Different Final States (32 Pillars)

Let the domain be $[0, 1]^2$ and the surface be **32 pillars** with $h = 0.15, a = b = 0.03$ and $\theta_Y = 110^\circ$



Cassie-1
to
Wenzel
(Marching)

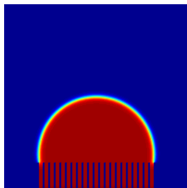


Cassie-1
to
Wenzel
(Showering)

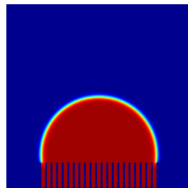
Cassie-1
to
Impregnated

Transitions to Different Final States (32 Pillars)

Let the domain be $[0, 1]^2$ and the surface be **32 pillars** with $h = 0.15, a = b = 0.03$ and $\theta_Y = 110^\circ$



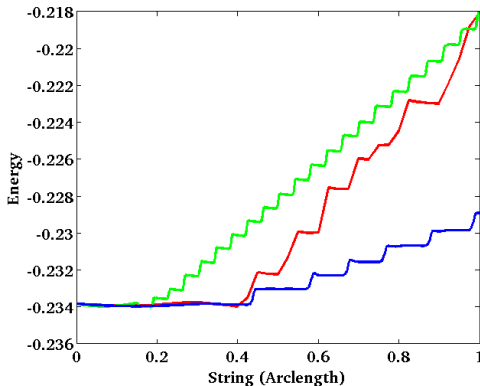
Cassie-1
to
Wenzel
(Showering)



Cassie-1
to
Wenzel
(Marching)

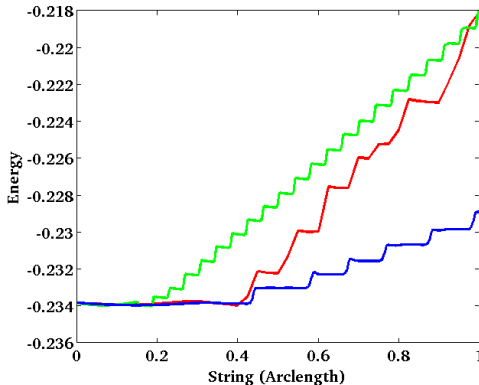
Cassie-1
to
Impregnated

Energy along MEPs (32 pillars)



Green: Cassie to Wenzel (Marching)
Red: Cassie to Wenzel (Showering)
Blue: Cassie to Impregnated

Energy along MEPs (32 pillars)



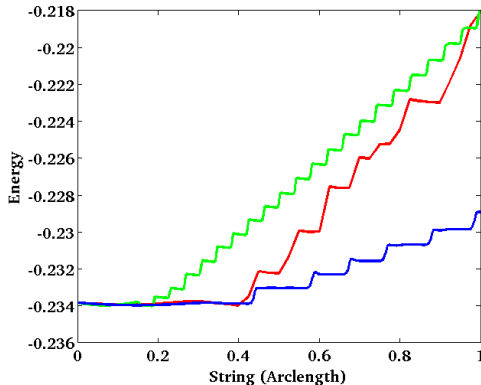
Green: Cassie to Wenzel (Marching)

Red: Cassie to Wenzel (Showering)

Blue: Cassie to Impregnated

- Green reaches a metastable state (of higher energy) each time a pore is filled

Energy along MEPs (32 pillars)



Green: Cassie to Wenzel (Marching)
Red: Cassie to Wenzel (Showering)
Blue: Cassie to Impregnated

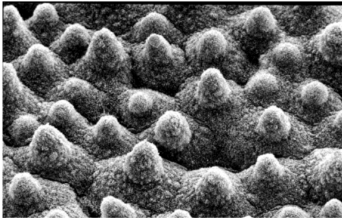
- Green reaches a metastable state (of higher energy) each time a pore is filled
- The Wenzel State has higher energy than the Cassie State

Increased Cassie State Stability

How do we increase the Cassie State Stability?

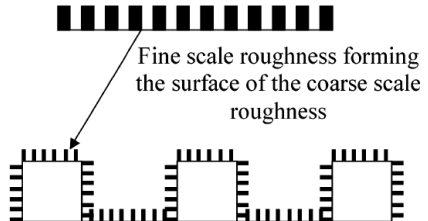
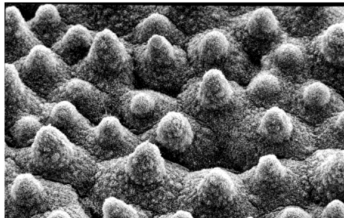
Increased Cassie State Stability

How do we increase the Cassie State Stability?



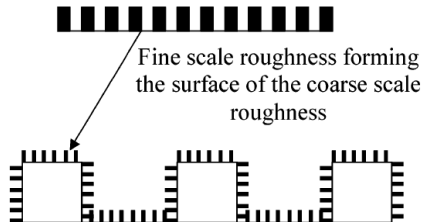
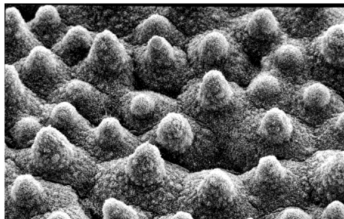
Increased Cassie State Stability

How do we increase the Cassie State Stability?



Increased Cassie State Stability

How do we increase the Cassie State Stability?

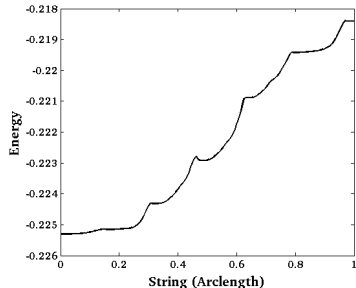


Introducing a hierarchy or roughness has been suggested:

- Patankar, Langmuir 20, 8209-8213 (2004) (includes above images)
- Bormashenko, Langmuir 27 8171-8176 (2011)
- Others...

Increased Cassie State Stability

Example of a Cassie-Wenzel transition on a surface with two scales of roughness

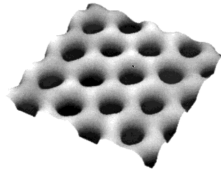


Increased energy barrier compared to the transitions shown earlier

Introduction to Chemically Structured Surfaces



Beetle Wings



Periodic Patterns

Top Left:

Parker & Lawrence Nature 414, 33 - 34 (2001)

Top Right:

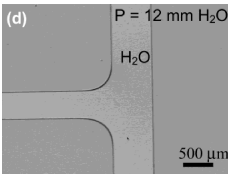
Lenz, et al. Langmuir 2001, 17, 7814-7822

Bottom Left:

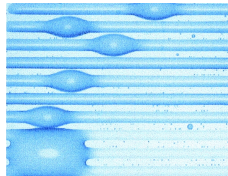
Zhao et al. Langmuir 2003, 19, 1873-1879

Bottom Right:

Gau, et al. Science 1999, 283, 46



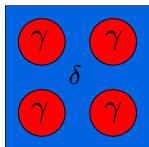
Microchannels



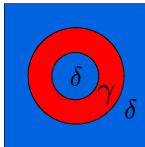
Striped Surfaces

Surface Structures

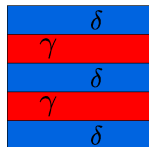
Experimentalists have developed methods to produce **chemically structured surfaces** with the following patterns



Regular Pattern of
Circular Domains



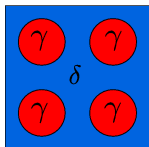
Ring-Shaped Domain



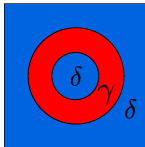
Striped Domains

Surface Structures

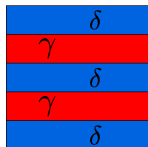
Experimentalists have developed methods to produce **chemically structured surfaces** with the following patterns



Regular Pattern of
Circular Domains



Ring-Shaped Domain



Striped Domains

*We will focus Striped Domains and Cross-Striped Domains

Metastable States

Lipowsky et al. have studied the morphological transitions of droplets on circular surface domains.

Metastable States

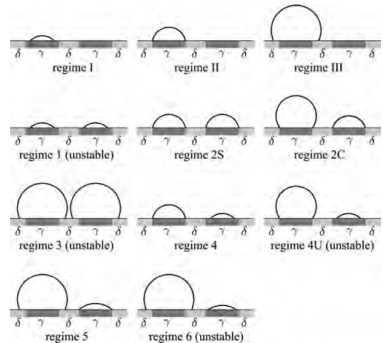
Lipowsky et al. have studied the morphological transitions of droplets on circular surface domains.

They found **11 permitted morphologies** for one or two droplet systems. By looking at the free energy of the system they derived a stability condition which gives **7 metastable or stable** droplet configurations

Metastable States

Lipowsky et al. have studied the morphological transitions of droplets on circular surface domains.

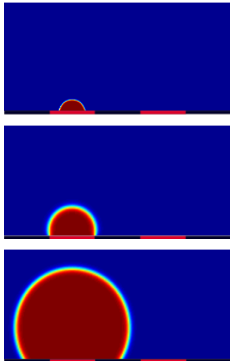
They found **11 permitted morphologies** for one or two droplet systems. By looking at the free energy of the system they derived a stability condition which gives **7 metastable or stable** droplet configurations



* Lipowsky et al. Langmuir 25(23), 12493 (2009)

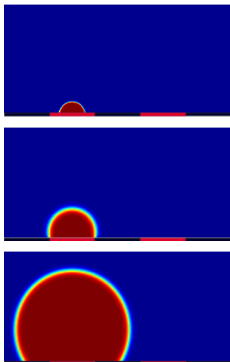
Metastable States

Using a two-dimensional model, we were able to recover the metastable and stable states that Lipowsky found as permissible.



Metastable States

Using a two-dimensional model, we were able to recover the metastable and stable states that Lipowsky found as permissible.



Pinning:

- If a droplet resides on the hydrophilic region: $\theta = \theta_\gamma$
- If a droplet is pinned at region interface:
 $\theta_\gamma \leq \theta \leq \theta_\delta$
- If a droplet extends to hydrophobic region:
 $\theta = \theta_\delta$

Different Transitions

We found to **modes of transitions** of 2D droplets in chemically patterned surfaces:

- By exchanging volume through the **vapor phases**
- By “**crawling**” over the hydrophobic region

Different Transitions

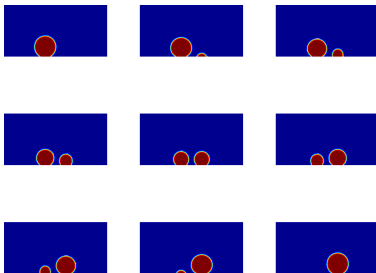
We found to **modes of transitions** of 2D droplets in chemically patterned surfaces:

- By exchanging volume through the **vapor phases**
- By “**crawling**” over the hydrophobic region

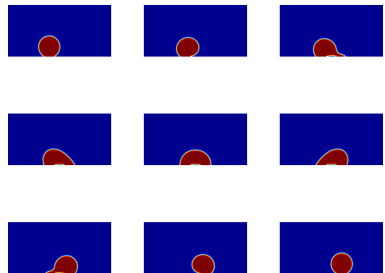
Given these two modes of transition, which is more likely?
What are the energy barriers associated with each transition?

Different Transitions

Here are pictures of the system at different points along the different minimum energy paths.

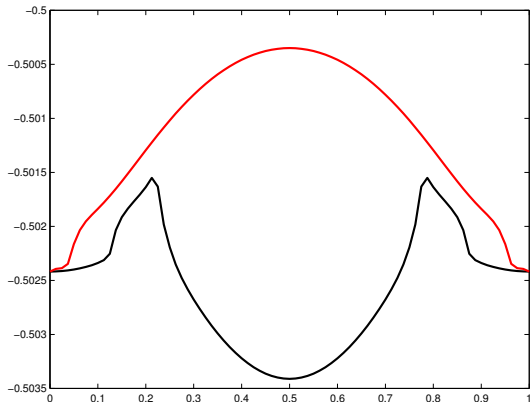


Transition through
vapor phase



Transition by
crawling

Different Transitions

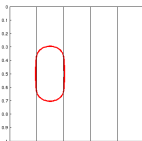
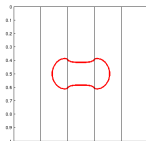
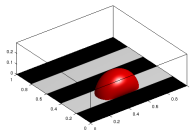
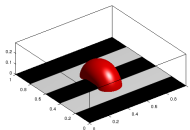


- Red: Transition through vapor phase
- Black: Transition by crawling
- Note that midpoint along the red MEP is unstable as Lipowsky predicts
- The midpoint along the black MEP is more stable than the endpoints of the MEP

Metastable States in Three Dimensions

There exist to simple metastable states that a droplet can reside in on a striped surface:

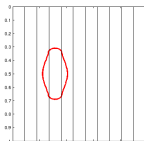
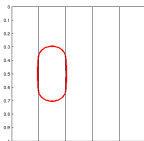
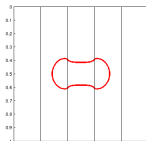
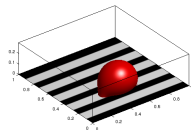
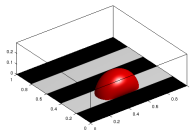
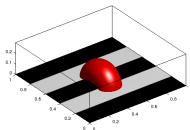
- Along one stripe (or chemical channel)
- Spread across three chemically patterned regions (bridge morphology)



Metastable States in Three Dimensions

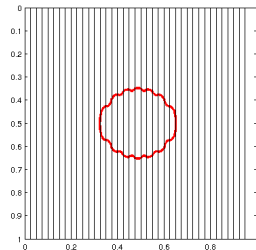
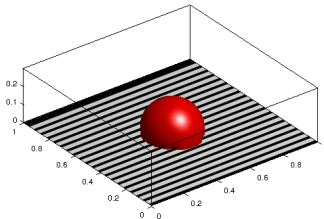
There exist to simple metastable states that a droplet can reside in on a striped surface:

- Along one stripe (or chemical channel)
- Spread across three chemically patterned regions (bridge morphology)



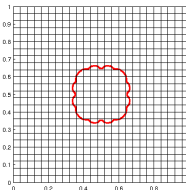
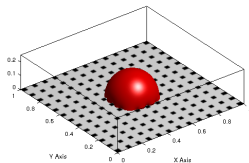
Metastable States in Three Dimensions

If the droplet is large and covers many chemically structured regions then we have a nice **spreading droplet** that fingers into the hydrophilic regions.



Rectangular Patterning

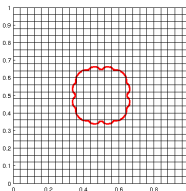
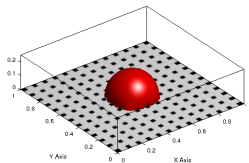
A common chemical structuring is rectangular patterning.



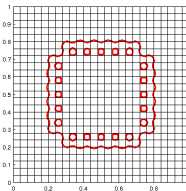
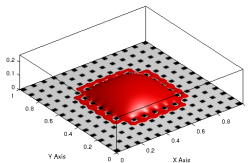
$$\begin{aligned}\theta_a &= 85^\circ \text{ (grey)} \\ \theta_r &= 130^\circ \text{ (black)} \\ a &= b = .04\end{aligned}$$

Rectangular Patterning

A common chemical structuring is rectangular patterning.



$$\begin{aligned}\theta_a &= 85^\circ \text{ (grey)} \\ \theta_r &= 130^\circ \text{ (black)} \\ a &= b = .04\end{aligned}$$

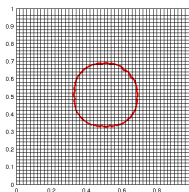
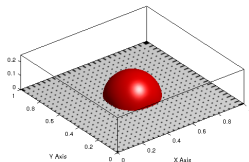


$$\begin{aligned}\theta_a &= 60^\circ \text{ (grey)} \\ \theta_r &= 130^\circ \text{ (black)} \\ a &= b = .04\end{aligned}$$

Note: Fingering occurs and “Islands” appear when θ_a is small

Rectangular Patterning

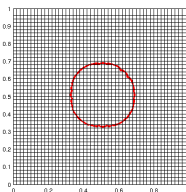
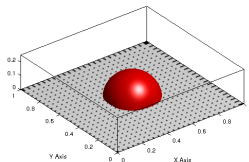
A common chemical structuring is rectangular patterning.



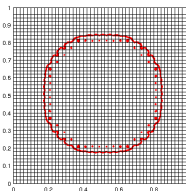
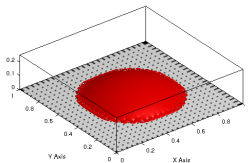
$$\begin{aligned}\theta_a &= 85^\circ \text{ (grey)} \\ \theta_r &= 130^\circ \text{ (black)} \\ a &= b = .02\end{aligned}$$

Rectangular Patterning

A common chemical structuring is rectangular patterning.



$$\begin{aligned}\theta_a &= 85^\circ \text{ (grey)} \\ \theta_r &= 130^\circ \text{ (black)} \\ a &= b = .02\end{aligned}$$



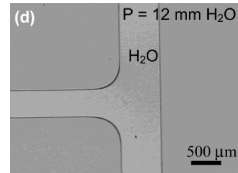
$$\begin{aligned}\theta_a &= 60^\circ \text{ (grey)} \\ \theta_r &= 130^\circ \text{ (black)} \\ a &= b = .02\end{aligned}$$

Microchannels

If chemical structure is on the scale of the droplet size then there are a number of useful applications including:

Microchannels

Surface-directed fluid flow
For use in microfluidic systems



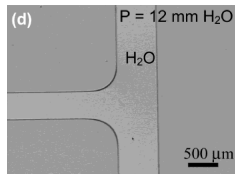
* Zhao et al. Langmuir 2003, 19, 1873-1879 (top)

Microchannels

If chemical structure is on the scale of the droplet size then there are a number of useful applications including:

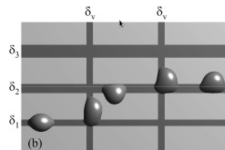
Microchannels

Surface-directed fluid flow
For use in microfluidic systems



Droplet Sorting

Helps control droplet size



* Zhao et al. Langmuir 2003, 19, 1873-1879 (top)

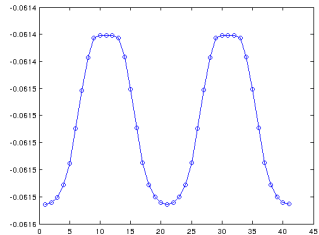
* Kusumaatmaja & Yeomans Langmuir 2007, 23, 6019-6032 (bottom)

Microchannels

If chemical structure is on the scale of the droplet size then there are a number of useful applications including:

$$\theta_a = 85^\circ, \theta_r = 115^\circ$$

width = .14

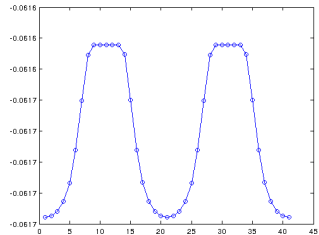


Microchannels

If chemical structure is on the scale of the droplet size then there are a number of useful applications including:

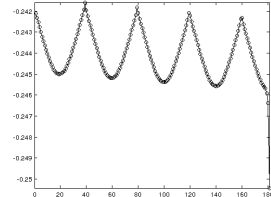
$$\theta_a = 85^\circ, \theta_r = 115^\circ$$

width = .10



Fluid Flow

Another example of the type of droplet that can be studied using our method.



$$\theta_a = 70^\circ, \theta_r = 120^\circ$$

Energy Plot along String

Note: Each energy minimum (left to right) decreases in energy



Conclusion

- We used a phase field model to study droplets on homogeneous, pillared, and chemically structured surfaces
- The String Method was used to find a variety of MEPs between Cassie-Baxter and Wenzel states
- We showed the increased energy from surfaces with double roughness
- We studied droplets on striped and rectangular patterned surfaces
- We demonstrated the string method use from studying surfaces designed for microfluidics

Future Work

- Study optimal conditions for pillared surface structure to enhance hydrophobicity
- Complete code that uses Adaptive-Mesh Refinement for 3D simulations
- Further explore the Energy Landscape for different methods of transitions corresponding to other minimal energy paths
- Apply the same methodology to liquid bridges and functional fibers

Acknowledgements

Acknowledgements:

- My advisor: Professor Weiqing Ren
- National Science Foundation
- MacCracken Fellowship Fund (NYU)
- Organizers of this conference

Thanks

Thanks!

Questions/Comments:
kellen@cims.nyu.edu